Comparative Study on The Stability of Hydropower Station Slope under Different Earthquake Conditions

wang zhongchang (wazoch@163.com)
Dalian Jiaotong University
Bo Li
Dalian Jiaotong University

Research Article

Keywords: seismic action, slope, different working conditions, dynamic response, stability

Posted Date: February 18th, 2021

DOI: https://doi.org/10.21203/rs.3.rs-206964/v1

Version of Record: A version of this preprint was published at Geotechnical and Geological Engineering on March 25th, 2021. See the published version at https://doi.org/10.1007/s10706-021-01780-5.

Abstract

In order to explore the stability characteristics of hydropower station slope under different working conditions under seismic action, The three-dimensional dynamic finite element method is used to analyze the working conditions of the hydropower station slope under the seismic load with a probability of exceeding 5% in 50 years, 2% in 100 years, and 1% in 100 years, through comparing the dynamic response characteristics and the stability of the slope under different seismic load were obtained. The results showed that under the influence of different earthquake loads, the ground motion response of the slope would increase with the increase of the peak value of the excited ground motion, and all would be forced to vibrate according to the vibration form of the excited ground motion; compared with the amplification effect of the slope on the displacement, the amplification effect of the slope on the acceleration was more obvious, this phenomenon was more obvious when the slope was under the action of an earthquake load with a probability of exceeding 1% within 100 years of the reference period; with the increase of seismic load, the possibility of bedding sliding and failure of the slope surface would be greater; when the three types of seismic loads act on the slope respectively, the other surfaces of the slope would generate instantaneous tensile stress, but they are less than the tensile strength of the slope rock mass. when the slope was under rare ground motion with a 100-year exceeding probability of 1% and 2%, the maximum relative dynamic displacement was about 5cm, and the slope was sufficient to withstand the test of strong ground motion; for the other two seismic conditions, when the slope was under the action of an earthquake load with a probability of exceeding 1% within 100 years of the reference period, the damage effect of the slope near the empty surface under the action of the earthquake was more obvious than that of the center of the slope.

1. Introduction

Due to the complex structure of the rock and soil that constitutes the slope of the hydropower station, the damage degree is very high(Ding et al. 2019), and in a certain earthquake area, the seismic activity has a certain periodicity(Xue et al. 2012), so under the action of strong earthquakes, the slope rock and soil is prone to sliding force, and in severe cases, it will cause landslides, which will affect the construction and operation of hydropower stations. Landslides caused by earthquakes are very harmful, so it is particularly important to ensure the stability of high and steep slopes of hydropower stations under strong earthquakes(Shen et al. 2016). At present, scholars at home and abroad have conducted a large number of studies on slope geological disasters caused by earthquakes, mainly including theoretical analysis of slope mechanics, indoor physical experiments to study the properties of slope soil, and numerical simulations, so as to analyze the overall mechanical stability of the slope under the action of earthquakes(Ping et al. 2015).Yang combined the geographic information system with the measured data, analyzed the influence of different factors on the distribution characteristics of the landslide before and after the earthquake, and established a binary Logistic regression model to analyze the susceptibility changes of the landslide before and after the earthquake to determine The area affected by earthquake action(2019); Biondi et al. used shaking table tests to study the ground motion response results of the model, and conducted corresponding analyses in both the time domain and frequency domain(2015); Zeng et al. took the rock collapse of rock slopes in western Hubei as the research object, combined field survey, engineering geological analysis and numerical numerical simulation analysis to study the collapse and collapse mechanism of slopes(2018); Fan et al. used the dynamic time history method to analyze the dynamics of the landslide under the action of ground motion loads by considering the dynamic characteristics of rock materials and seismic characteristics, and selected the minimum average stability coefficient as the evaluation result(2010); Huang analyzed the influence of horizontal and vertical seismic action on slope stability by using the finite element strength reduction method, and quantitatively analyzed the necessity of considering seismic action in different areas(2020); Fan et al. analyzed the earthquake landslide and pointed out that the fault and the aspect position jointly determine the average slope of the landslide and the earthquake throwing effect (2012).Taking the slope engineering of a large hydropower station as an example, this study used different peak accelerations to analyze the evolution of the slope response to earthquakes of different intensities, and provides a reasonable basis for the improvement of the seismic performance of the powerhouse slope of the hydropower station(Zhan et al. 2019)

2. Engineering Geology

A hydropower station project is located in an area of high seismic intensity. It consists of riverbed concrete face rockfill dams, ground powerhouses, power plant diversion and power generation systems, flood discharge tunnels, and empty tunnels. It has the characteristics of many passways and large flood discharge. The geological conditions of the area where the hydropower station is located are complex, with many large faults and structural planes distributed; the slope has high ground stress, and the unloading phenomenon is serious after excavation; and the surface rock mass structure of the slope is unstable, which is prone to slippage under the action of dynamic load. Because the safety of the slope structure under the action of seismic load plays a vital role in the safe operation of the entire hydropower station, this article was based on the three-dimensional numerical analysis method, using finite element programs and using time history analysis to study the dynamic characteristics and seismic response of the hydropower plant slop under different seismic load conditions, in order to have a good understanding of stability of the hydropower station slope under seismic loads(Ding et al. 2018), and provided some conceptual guidance for the seismic design of hydropower stations and their slope structures

3. The Establishment Of Slope Calculation Model And Parameter Selection

The three-dimensional finite element slope model was established as shown in Figure 1 , and the calculation range was 350m×285m×450m, and the foundation was regarded as a massless elastic element. Before calculation, static and dynamic boundary conditions needed to be applied to the model. Among them, the static boundary conditions imposed were: horizontal constraints were imposed on the outer edge of the slope, and normal constraints were imposed on the bottom. The slope surface and the open surface of the spillway tunnel were free boundaries; the dynamic boundary conditions were the viscous boundary and free field boundary in ANSYS , the load was dynamically input in the form of interaction force at the boundary. The slope of the hydropower station was set as a three-dimensional solid element model to perform a three-dimensional finite element dynamic response analysis.

During the calculation process, the rock mass and concrete were regarded as ideal linear elastic materials, the dynamic elastic modulus of the material was taken as 1.3 times of the static elastic modulus, and the Drucker-Prager yield criterion is adopted; the stress field was regarded as the initial ground stress field, and the dynamic deformation modulus and dynamic Poisson's ratio used were the changed values(Guo et al. 2013). The selected physical and mechanical parameters are shown in Table 1.

Table 1 Physical and mechanical parameters of slope rock mass and lining structure

Rock layers category	Density (kN/m^3)	Rock saturated compressive strength (MPa)	Dynamic deformation modulus (GPa)	Dynamic Poisson's ratio	Critical damping ratio
Complete andesite	2650	70–80	25.87	0.32	0.05
Broken andesite	2550	60–70	7.54	0.39	0.05
Mud shale	2200	60	0.533	0.47	0.05
Sandstone	2500	35–40	1.95	0.42	0.05
Paleo weathered rock	2200	15–20	0.845	0.47	0.05
C25 concrete	2518		33.8	0.163	0.05

4. The Selection Of Seismic Waves

In this paper, the time history analysis method was used to input the acceleration history curve of seismic motion into the established slope model, so as to perform the displacement, stress and acceleration response of the plant slope during the earthquake(Pan et al. 2010). While selecting the seismic wave load, the impact of tectonic stress was not considered for the time being, and the seismic acceleration in the downstream, transverse and vertical directions were respectively considered for simulation. The calculation time of ground motion was 20s.The acceleration time history adopted the peak acceleration time history of ground motion with a probability of exceeding 5% within 50 years, 2% within 100 years and 1% within 100 years in the reference period, as shown in Figure 2-Figure 4(The horizontal axis represented time, unit: s; the vertical axis represented acceleration, unit: g) .While selecting the acceleration of the seismic load, 2/3 of the acceleration in the direction of the tunnel axis was regarded as the vertical acceleration, and the acceleration along the tunnel axis was taken as the acceleration along the depth direction.

5. Analysis Of Slope Dynamic Response

5.1 Analysis of slope stress law

After the excavation of the side slope of the plant was completed, finite element simulation and analysis under different seismic conditions were carried out. When seismic waves of different wave forms were applied to the slope, the distribution diagram of the maximum time history of the first principal stress was shown in Figure 5, and the third principal stress corresponding to the maximum time history of the first principal stress was shown in Figure 6.

Figure 5 showed the maximum time-history distribution of the first principal stress of the slope under seismic loads with a probability of exceeding 5% within 50 years, 2% within 100 years and 1% within 100 years in the base period. Figure 6 showed the time history distribution diagram of the third principal stress corresponding to the maximum value of the first principal stress time history under three different seismic conditions.It could be seen from Figure 5 and Figure 6 that when the slope was in the process of seismic loading with a probability of exceeding 5% within 50 years of the reference period, the maximum tensile stress generated occurred at the entrance of the diversion tunnel and was 0.25 MPa; when the slope was in the process of seismic loading with a probability of exceeding 2% within 100 years in the reference period, the maximum tensile stress generated occurred at the bottom of the sandstone, which was 0.52MPa; when the slope was in the process of seismic loading with a probability of exceeding 1% within 100 years of the reference period, the maximum tensile stress appears on the top surface of the slope near the boundary, and its value was 0.346 MPa.

5.2 Analysis of slope displacement law

After the slope excavation of the workshop was completed, when it was under seismic loads in different working conditions, the displacement of the slope in X, Y and Z directions was shown in Fig. 7-9 when the time history of the first principal stress was the maximum.

It could be seen from Figures 7-9 that when the slope was under different seismic conditions, the maximum uplift deformation of the slope along the vertical direction appeared on the surface of the rock near the foot of the slope, and the values were 2.0cm and 4.46cm, 4.31cm respectively; the deformation of the slope along the tunnel axis appeared in the middle of the shale. When the slope was under the action of an earthquake load with a probability of exceeding 5% within 50 years of the reference period, the maximum deformation of the slope along the tunnel axis was 1.5 cm, which was the minimum value of the three working conditions. At this time, the slope rock mass had obvious signs of failure; the maximum deformation of the slope along the tunnel axis occurred when the slope was under the action of an earthquake load with a probability of exceeding 2% within 100 years of the reference period. The maximum value was 5.8cm. At this time, It was more likely that the slope was sliding along the bed.

5.3 Analysis of dynamic response at foot of side slope

5.3.1 Time history analysis of dynamic displacement at slope foot

After the excavation of the plant slope was completed, when the first principal stress time history was the maximum under the action of the seismic load of different working conditions, the X, Y and Z directions corresponding to the center of the slope toe at an elevation of 94.8m The displacement was shown in Figure 7-9, and the dynamic displacement time history curve was shown in Figure 10-12.Under the action of ground motions with a probability of exceeding 5% in 50 years, 2% in 100 years and 1% in 100 years in the reference period, the maximum relative dynamic displacement in the X direction at the center of the foot of slope was close to 1.5cm, 2.8cm, and 3.2cm respectively; the maximum relative dynamic displacement in the Y direction at the center of the foot of slope was close to 1.4cm, 3.5cm, and 3.9cm, respectively; the maximum relative dynamic displacement in the Z direction at the center of the foot of slope was close to 1.5cm, 2.8cm, and 3.1cm respectively.Through comparison, it could be obtained that under the action of the seismic load with a probability of 1% of the slope in the reference period of 100 years, the displacements in all directions were larger than those of the other two working conditions; under three different seismic working conditions , the foot of slope at an elevation of 94.8m was less likely to be damaged under the action of ground motions.

5.3.2 Analysis of rock mass acceleration at slope foot

Under the action of ground motions with a probability of exceeding 5% in 50 years, 2% in 100 years and 1% in 100 years in the reference period, the rock slopes all perform similar forced vibrations in the form of exciting ground motions. The acceleration time history curve of the rock mass at the center of the slope foot at an elevation of 94.8m was shown in Figure 13-Figure 15.Under three different seismic loads, the maximum acceleration of rock mass at the central slope foot along the X direction was 0.87m/s^2,1.6m/s^2 and 1.6m/s^2, the maximum acceleration along the Y direction was 0.62m/s^2,1.3m/s^2 and 1.4m/s^2, and the maximum acceleration along the Z direction was 0.8m/s^2,1.3m/s^2 and 1.55m/s^2.By comparison, it could be found that the acceleration of slope rock mass in all directions was larger than the displacement of the other two working conditions under the seismic load with a probability of exceeding 1% in 100 years in the reference period.According to the analysis of the slope dynamic acceleration, the possibility of failure at the slope foot at the elevation of 94.8m was relatively small under the action of three kinds of ground motion.

5.3.3 Stress seismic response analysis of rock mass at slope foot

Under the action of ground motions with a probability of exceeding 5% in 50 years, 2% in 100 years and 1% in 100 years in the base period, the maximum compressive stress of the rock mass at the center of the slope foot at an elevation of 94.8m was close to 0.24MPa,0.56MPa and 0.7MPa respectively, the maximum tensile stress was close to 0.27MPa, 0.52MPa and 0.7MPa respectively.By comparing the maximum tensile stress and compressive stress at the foot of the slope under three seismic conditions, it could be obtained: under the action of ground motion with a probability of 1% in the reference period within 100 years, the value of tensile stress generated by the rock mass at the toe of the slope and the compressive stress values were all the maximum values; under three different seismic conditions, the possibility of failure of the rock mass at the foot of the slope was relatively small.

By analyzing and comparing the displacement distribution, stress distribution and dynamic response characteristics of the rock mass at the foot of the slope under three different ground motions, it could be found that the rock mass at the foot of slope was most obviously affected by the ground motion, which 1% probability of exceeding within 100 years of the reference period; under different seismic conditions, the slope rock mass structure was generally in a stable state.

5.4 Analysis of ground motion response at other positions of slope

Based on the analysis method of the dynamic response at the foot of the slope, the slope was simulated under the action of ground motion with the probability of exceeding 5% within 50 years of the reference period, 2% within 100 years, and 1% within 100 years. The characteristics of dynamic displacement time history, rock mass acceleration, rock mass stress and seismic response at the center, the center of the slope top surface, and the slope top surface near the center of the side

slope. The analysis showed that different positions of the slope were under different seismic load conditions. The following variable values are shown in Table 2.

Table 2 Variable values at different locations under various seismic conditions

Working condition	location	The maximum stress (MPa)		The maximum displacement (cm)			The maximum acceleration (m/s^2)		
		compressive stress	tensile stress	in X direction	in Y direction	in Z direction	in X direction	in Y direction	in Z direction
Exceeding 5% within 50 years	The foot of slope	0.24	0.27	1.5	1.4	1.5	0.87	0.62	0.8
	The Center of slope	0.16	0.17	1.62	1	1	0.83	0.45	0.7
	The center of the top of the slope	0.16	0.16	1.9	1	1	1.05	0.42	0.58
	the top surface near the side slope	0.06	0.07	2	1	1	1.05	0.41	0.6
Exceeding 2% within 100 years	The foot of slope	0.56	0.53	2.8	3.5	2.8	1.6	1.3	1.3
	The Center of slope	0.34	0.39	3.6	2.1	1.7	1.7	0.72	1
	The center of the top of the slope	0.35	0.35	4.5	2.3	1.3	2.2	0.85	0.9
	the top surface near the side slope	0.13	0.13	5	2.1	1.3	2.3	0.73	0.82
Exceeding 1% within 100 years	The foot of slope	0.7	0.7	3.2	3.9	3.1	1.6	1.4	1.55
	The Center of slope	0.42	0.45	3.6	2.8	1.9	1.8	1	1.05
	The center of the top of the slope	0.38	0.4	4.6	2.6	1.9	1.8	1	1.15

	the top surface near the side slope	0.15	0.16	5	2.7	1.25	2.42	1	1.2

By comparing the variable values at different positions of the slope under different seismic load conditions and combining with the data in Table 2, it could be concluded that:

(1)Under different seismic loads, the ground motion response of the slope would increase with the increase of the peak value of ground motion, and the slope would be forced vibration in accordance with the vibration form of induced ground motion;

(2)The stress, displacement and ground motion response characteristics of the slope were more obvious than those of the other two conditions when the slope is subjected to the rare earthquake with the probability of exceeding 5% within 50 years of the reference period. The maximum tensile stress on the slope surface is 0.7MPa, which was less than the tensile strength of the slope rock mass. Moreover, the maximum displacement on the surface of the slope was 5.8cm, which was less than the maximum displacement allowed by the slope rock mass, so the slope could withstand the action of strong earthquakes(Wen et al. 2016).

(3)The acceleration of ground motion at the side of the top slope was more obvious than that at the center of the top surface. In the rare earthquake with the probability of exceeding 5% within 50 years of the reference period. The failure effect of the side slope near the open surface was more obvious than that at the center of the top.

6. Conclusion

In this paper, by simulating the working conditions of the slope of hydropower station under the seismic load of the probability of exceeding 5% within 50 years, 2% within 100 years and 1% within 100 years in the reference period, the dynamic response characteristics of the slope at different positions under various seismic conditions were obtained, and the comparison and analysis were made. The analysis results showed that under different seismic conditions, the ground motion response of the slope would increase with the increase of the peak of the excited ground motion, and all would be forced to vibrate according to the vibration form of the excited ground motion; the amplification effect of the slope on the acceleration was more obvious than the amplification effect on the displacement. This phenomenon was more obvious when the slope was under the seismic load with a probability of exceeding 1% within 100 years of the reference period; as the seismic load increases, the more likely it was that the surface of the slope would slide along the bed and be damaged; when the slope was under the action of rare ground motions with a 100-year exceeding probability of 1% and 2%, the maximum relative dynamic displacement and maximum tensile stress generated by the slope were both within the allowable range of the slope rock mass, and the slope could withstand the test of strong earthquake and ground motion; when the slope was under the action of an earthquake load with a probability of exceeding 1% within 100 years of the reference period, the damage effect of the slope near the empty surface under the action of the earthquake was more obvious than that of the center of the slope.

Declarations

Acknowledgements

This work was supported by the National Natural Science Foundation of China (51774199) and Excellent Talents Fund Program of Higher Education Institutions of Liaoning Province (No. LR2018053) .

References

1. BIONDI G, MASSIMINO MR, MAUGERI M. (2015) Experimental Study in the Shaking Table of the Input Motion Characteristics in the Dynamic SSI of a SDOF Model. Bulletin of Earthquake Engineering,13(6):1835-1869.
2. Ding H G, Zhang Y J, Chen M B, et al. (2019) Analysis and Treatment Research of Landslide. Construction Technology,48(S1): 1100-1103**(in Chinese)**
3. Ding J H, Wang L, Deng H, Fan Y S,Tu G X. (2018) Influence from dominant structural plane of a hydropower station on Lancangjiang River on instability failure of rock slope.Water Resources and Hydropower Engineering,49(2):144-151**(in Chinese)**
4. Fan X Y,Zhang Y Y,Yang J R. (2012) Developmental characteristics and influence factors of landslides in Wenchuan earthquake.
Journal of Natural Disasters,(1):128-134**(in Chinese)**
5. Fan Z P, Zhang L H. (2010) Stability Analysis of Slope under Earthquake Action.Geotechnical Engineering Technique,24(01): 32-35.**(in Chinese)**
6. Guo S S, Li D Y. (2013) The effect of dynamic elastic modulus changes on the dynamic response of arch dams.Journal of China
7. Institute of Water Resources and Hydropower Research,11(2):125-129 **(in Chinese)**
8. Huang X. (2020) Finite Element Study of the Influence of Horizontal and Vertical Sake on the Slope Stability.Soil Engineering and Foundation,34(1):69-72**(in Chinese)**
9. Pan J W, Zhang C H, Xu Y J. (2010) The influence of strong earthquake input method and foundation model on gravity dam response. Chinese Journal of Geotechnical Engineering,32(1):82-87 **(in Chinese)**
10. Ping T Q, Luo X Q, Zheng A X. (2015) Stability under seismic loading Analysis of influence of cracks on rock slope. Rock and Soil Mechanies,36(2):600-606**(in Chinese)**
11. Shen B,Tang H, Wu Z J. (2016) Dynamic stability evaluation and reinforcement effect analysis of high-steep rock slope under earthquake. China Rural Water and Hydropower,(6):182-186,189**(in Chinese)**
12. Wen S C, Z J,Huang H W. (2016) Reliability Analysis of Soil High Slope Stability under Strong Seismic Condition. Chinese Journal of Solid Mechanics,37(S1):16-22**(in Chinese)**
13. Xue Y, Zhu Y Q, Yin J Y et al. (2012) Analysis on Seismicity Periods of Great Earthquakes in Japan. Earthquake,32(3):67-77 **(in Chinese)**
14. Yang D X. (2019) Comprehensive study on landslide susceptibility evaluation and seismic effect before and after earthquake in Qiaojia County, Yunnan Province. Kunming: Kunming University of Science and Technology**(in Chinese)**
15. Zeng R, Jiang M S, Sun L K, et al. (2018) Toppling failure mechanism of rock slope induced by heavy rainfall:a case study of the Zhaojiayan Rockfall in Western Hubei.The Chinese Journal of Geological Hazard and Control,29(3):12-17**(in Chinese)**
16. Zhan Z F, Qi S W, He N W, Zheng B W, Ge C F. (2019) Shaking table test study on homogeneous rock slope model under strong earthquake.Journal of Engineering Geology,27(5): 946-954**(in Chinese)**

Figures

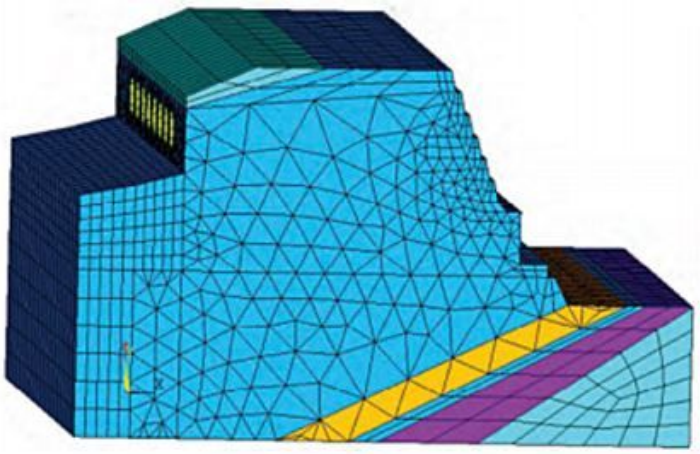

Figure 1

Calculation model of slope tunnel

Figure 2

Seismic wave forms that beyond the probability of 5% in 50 years

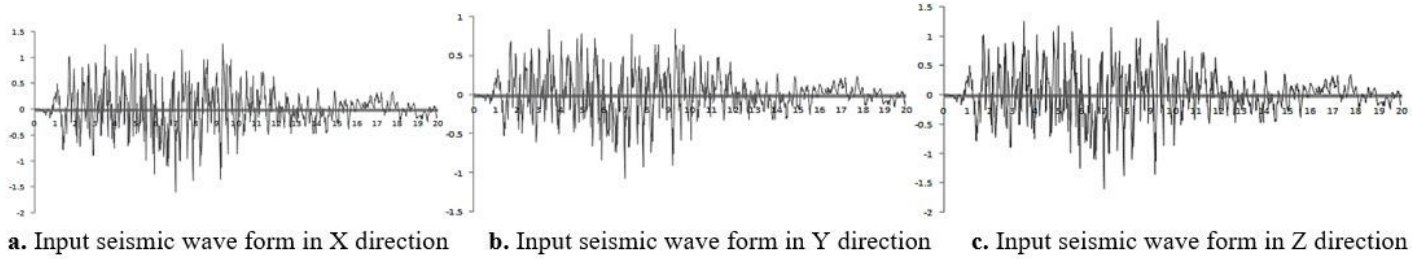

Figure 3

Seismic wave forms that beyond the probability of 2% in 100 years

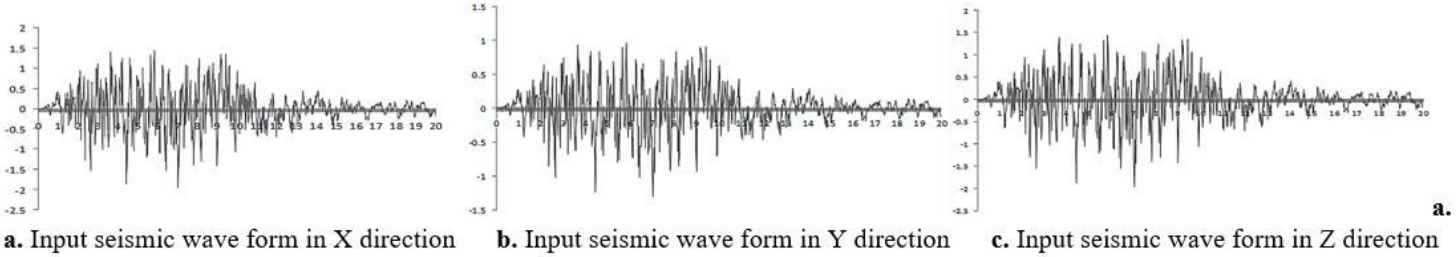

Figure 4

Seismic wave forms that beyond the probability of 1% in 100 years

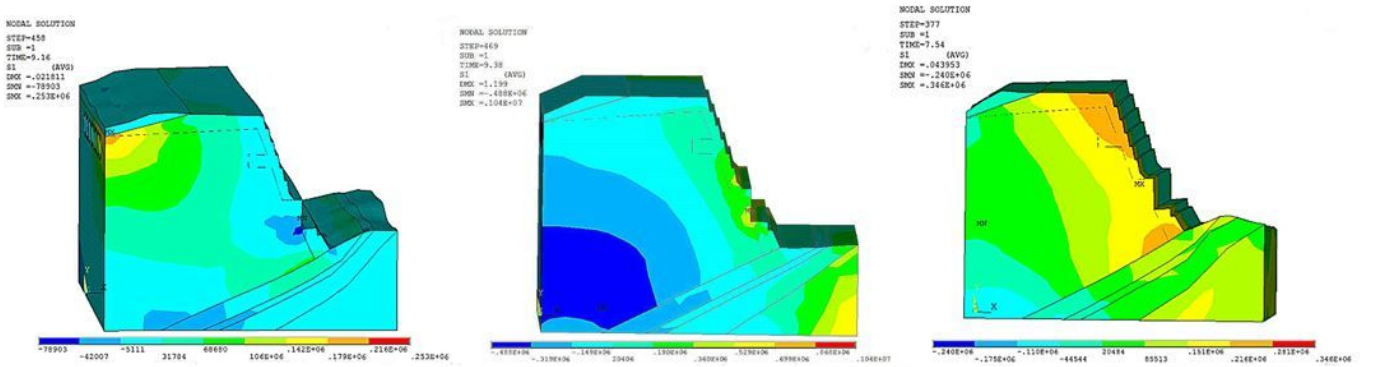

a. The distribution diagram of the maximum time history of the first principal stress (exceeding 5% within 50 years)

a. The distribution diagram of the maximum time history of the first principal stress (exceeding 2% within 100 years)

a. The distribution diagram of the maximum time history of the first principal stress (exceeding 1% within 100 years)

Figure 5

The distribution diagram of the maximum time history of the first principal stress under different seismic conditions

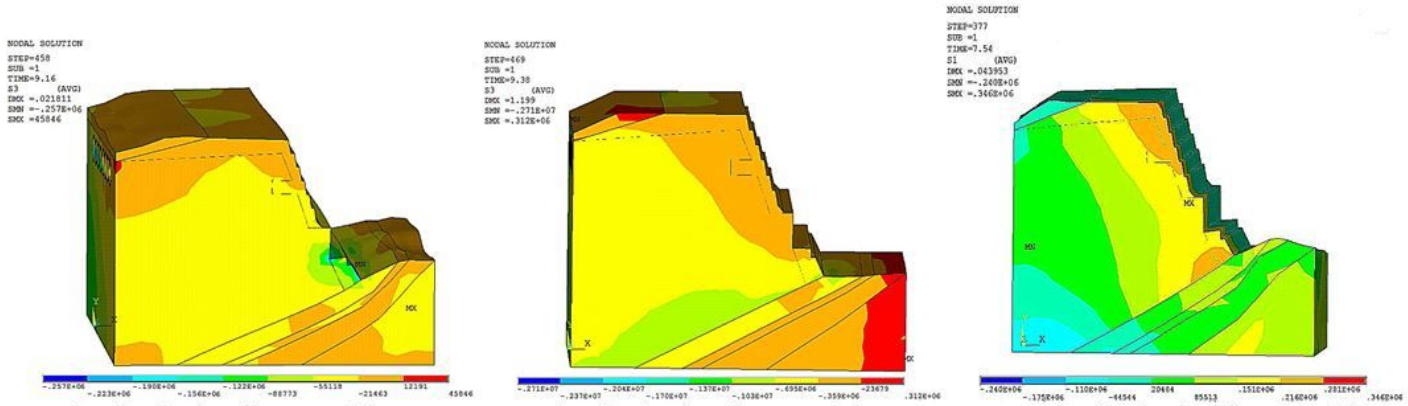

a. The distribution diagram of the maximum time history of the third principal stress (exceeding 5% within 50 years)

a. The distribution diagram of the maximum time history of the third principal stress (exceeding 2% within 100 years)

a. The distribution diagram of the maximum time history of the third principal stress (exceeding 1% within 100 years)

Figure 6

The distribution diagram of the maximum time history of the third principal stress under different seismic conditions

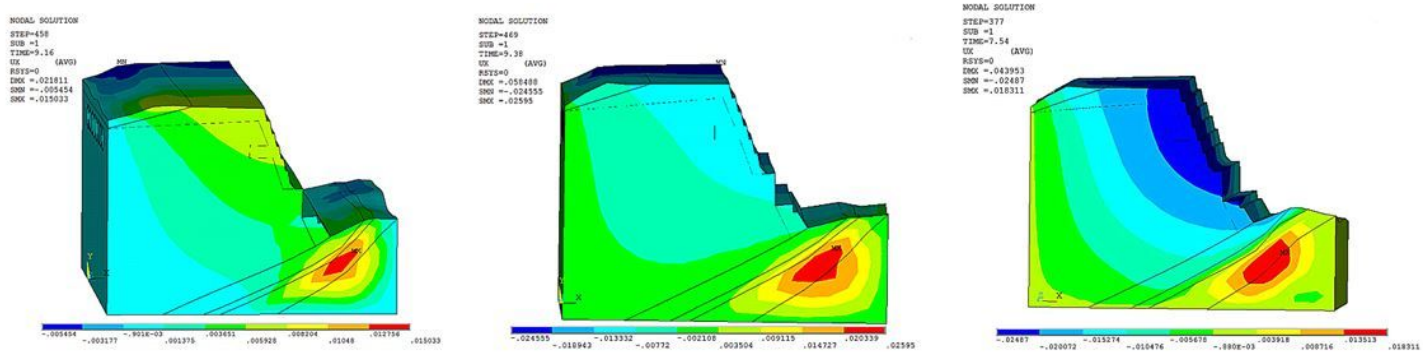

a.Displacement distribution in the X direction (exceeding 5% within 50 years)

b. Displacement distribution in the X direction (exceeding 2% within 100 years)

c. Displacement distribution in the X direction (exceeding 1% within 100 years)

Figure 7

Displacement distribution in X direction at maximum time history of the first principal stress under different seismic conditions

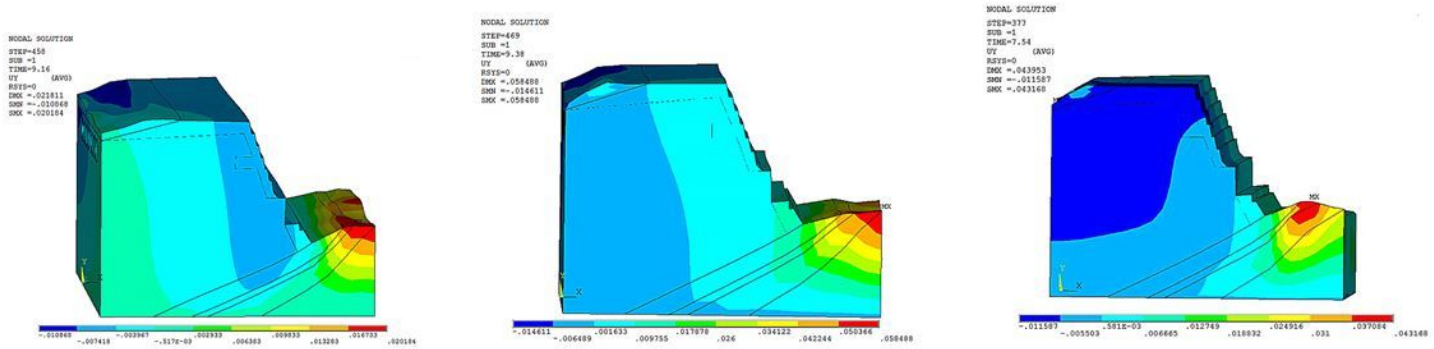

a.Displacement distribution in the Y direction (exceeding 5% within 50 years)

b. Displacement distribution in the Y direction (exceeding 2% within 100 years)

c. Displacement distribution in the Y direction (exceeding 1% within 100 years)

Figure 8

Displacement distribution in Y direction at maximum time history of the first principal stress under different seismic conditions

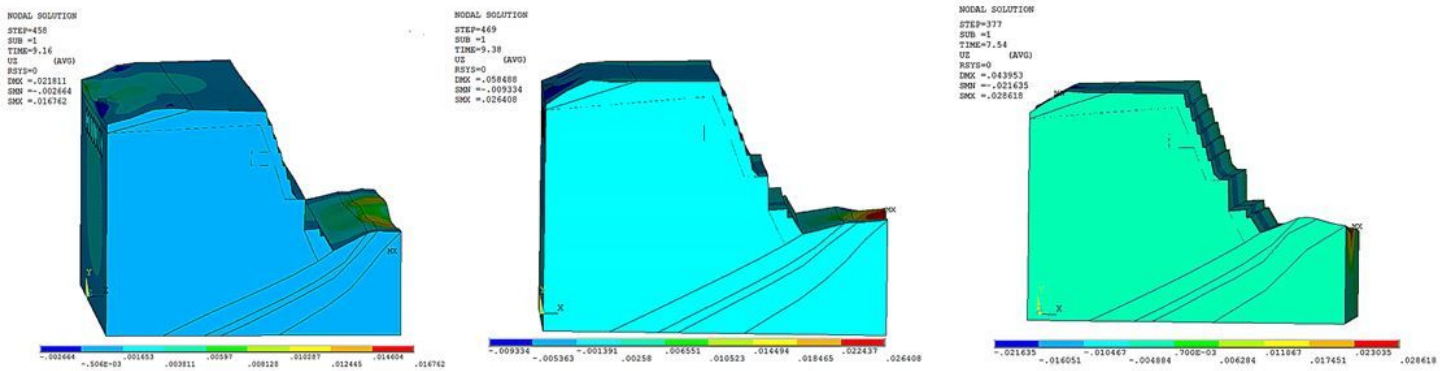

a.Displacement distribution in the Z direction (exceeding 5% within 50 years)

b. Displacement distribution in the Z direction (exceeding 2% within 100 years)

c. Displacement distribution in the Z direction (exceeding 1% within 100 years)

Figure 9

Displacement distribution in Z direction at maximum time history of the first principal stress under different seismic conditions

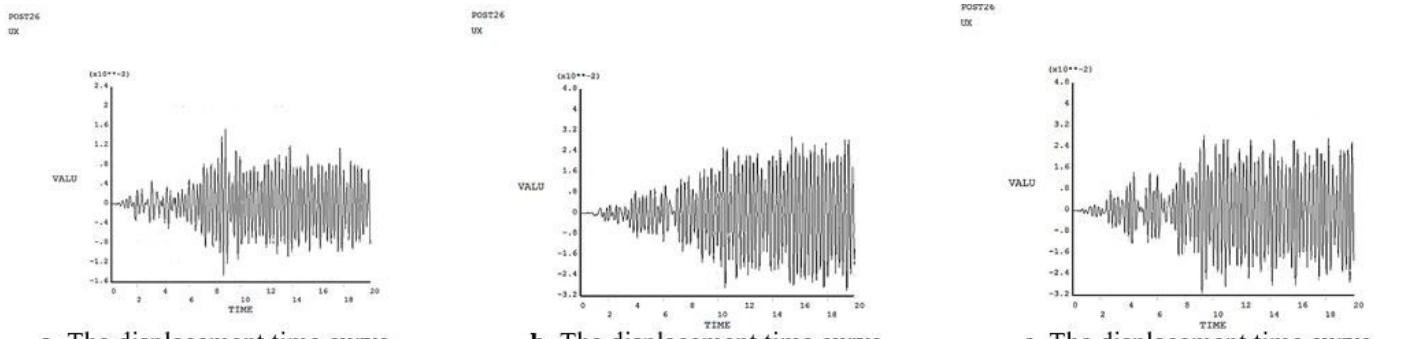

a. The displacement time curve in X direction (exceeding 5% within 50 years)

b. The displacement time curve in X direction (exceeding 2% within 100 years)

c. The displacement time curve in X direction (exceeding 1% within 100 years)

Figure 10

The displacement time curve in X direction at slope foot under different seismic conditions

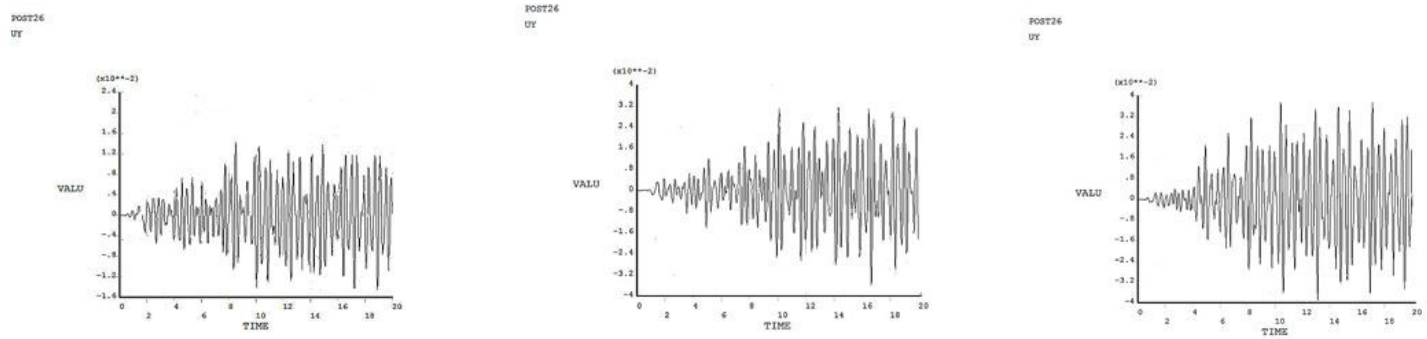

a. The displacement time curve in Y direction (exceeding 5% within 50 years)

b. The displacement time curve in Y direction (exceeding 2% within 100 years)

c. The displacement time curve in Y direction (exceeding 1% within 100 years)

Figure 11

The displacement time curve in Y direction at slope foot under different seismic conditions

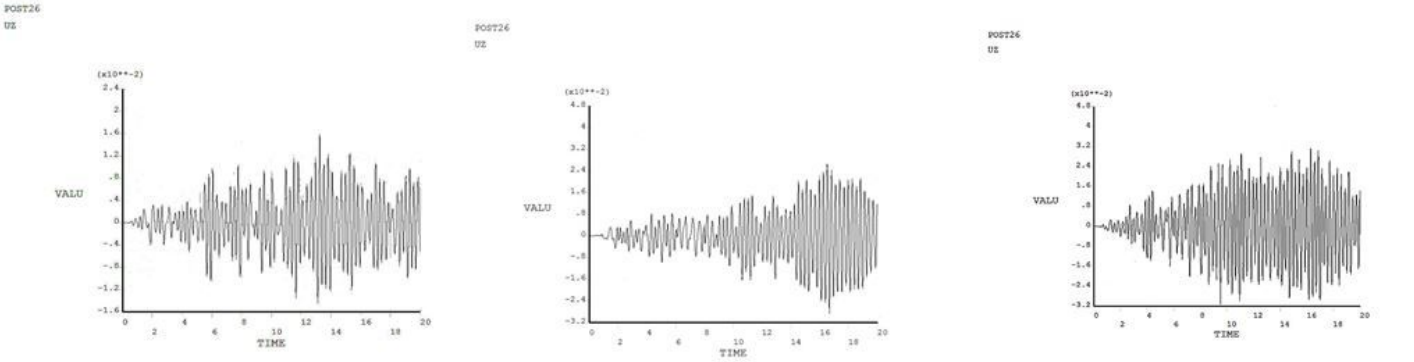

a. The displacement time curve in Z direction (exceeding 5% within 50 years)

b. The displacement time curve in Z direction (exceeding 2% within 100 years)

c. The displacement time curve in Z direction (exceeding 1% within 100 years)

Figure 12

The displacement time curve in Z direction at slope foot under different seismic conditions

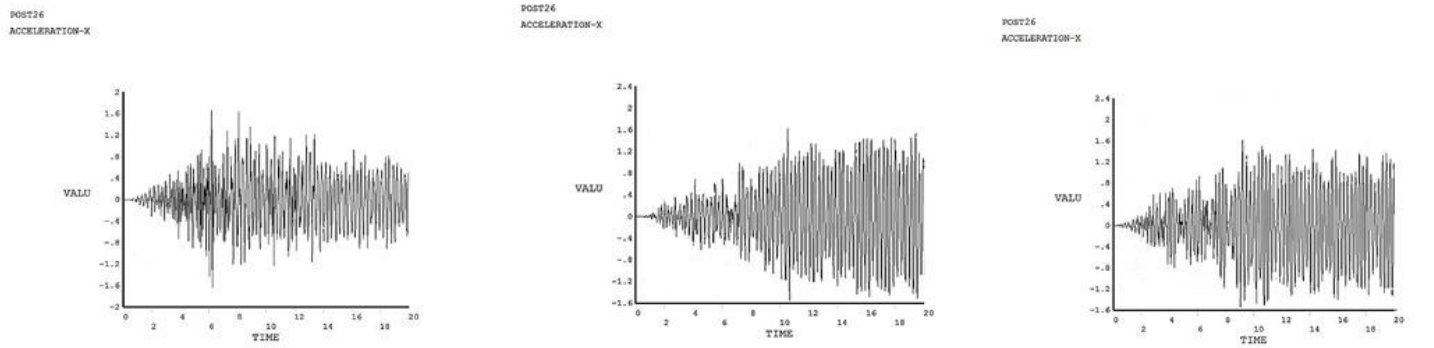

a.Curve of acceleration in X direction

b.Curve of acceleration in X direction

c.Curve of acceleration in X direction

Figure 13

The Curve of acceleration in X direction at slope foot under different seismic conditions

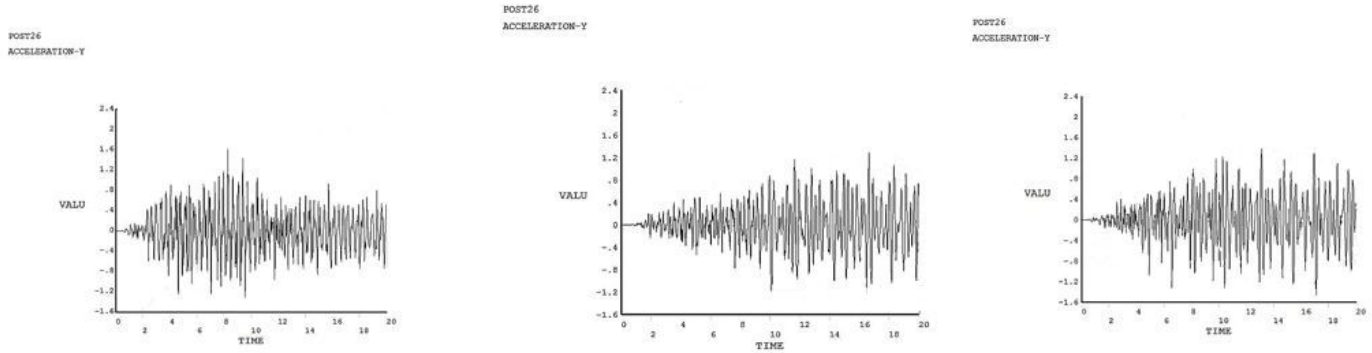

a.Curve of acceleration in Y direction b.Curve of acceleration in Y direction c.Curve of acceleration in Y direction

Figure 14

The Curve of acceleration in Y direction at slope foot under different seismic conditions

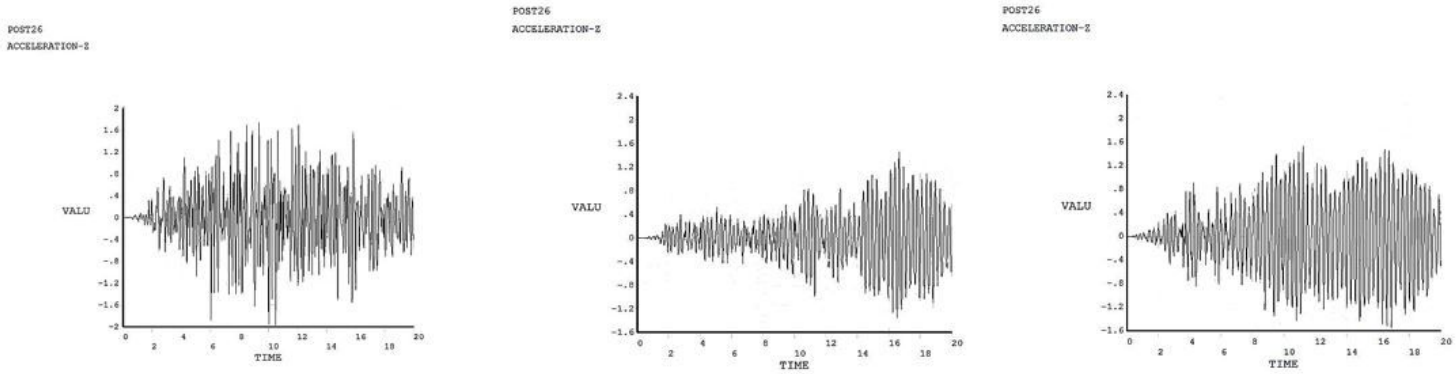

a.Curve of acceleration in Z direction b.Curve of acceleration in Z direction c.Curve of acceleration in Z direction

Figure 15

The Curve of acceleration in Z direction at slope foot under different seismic conditions

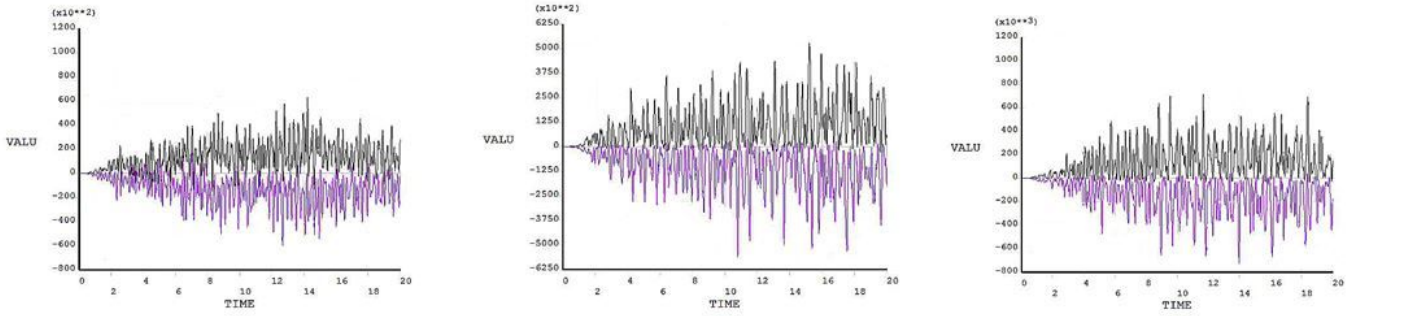

a. Time history curves of the first and third principal stresses

b. Time history curves of the first and third principal stresses

c. Time history curves of the first and third principal stresses

Figure 16

Time history values of the first and third principal stresses at the foot of slope under different seismic conditions